Noname manuscript No.
(will be inserted by the editor)

A Hierarchical modified AV1 Codec for Compression Cartesian form of Holograms in Holo and Object planes

Vahid Hajihashemi, Faculdade de Engenharia, Universidade do Porto, Portugal
Abdoreza Alavi Gharahbagh, Faculdade de Engenharia, Universidade do Porto, Portugal
Azam Bastanfard, Islamic Azad University, Karaj Branch, Iran
Hugo S. Oliveira, Faculdade de Engenharia, Universidade do Porto, Portugal
Gonçalo Almeida, Faculdade de Engenharia, Universidade do Porto, Portugal
Zhen Ma, Faculdade de Engenharia, Universidade do Porto, Portugal
João Manuel R. S. Tavares, Instituto de Ciência e Inovação em Engenharia Mecânica e Engenharia Industrial, Departamento de Engenharia Mecânica, Faculdade de Engenharia, Universidade do Porto, Portugal

Received: date / Accepted: date

Abstract Three-dimensional (3D) image reconstruction is emerging as a leading challenge for 3D media on the Internet and virtual reality. In this regard, compression performance in 3D technology is one of the most important issues. Various codecs such as HEVC and AV1 have been suggested to improve compression performance in 3D technology. In this study, a hybrid method based on AV1 codec combined with mathematical methods is proposed for improving the quality of this codec. In the proposed method, two AV1 compression

Corresponding author: Vahid Hajihashemi
R. Dr. Roberto Frias s/n, 4200-465 Porto
Tel.: +351-96-1700648
Fax: +351 22 508 1445
E-mail: Hajihashemi.vahid@ieee.org

steps are used to estimate the AV1 codec error using a linear relationship and added to the basic codec output to improve the compression performance. The proposed method shows better quality in the Cartesian form (real and imaginary parts) of the hologram in Holo and Object plane when compared to new codecs that have been proposed in the field of 3D compression. In addition, the proposed method can be used as a general compression method for 2D images. Based on simulation results, the proposed method improved the quality of reconstructed hologram by up to 63% and 5 dB in terms of BDRate and BDPSNR, respectively.

Keywords Compression · Digital Holography · AV1 · Wavelet · Interpolation

1 Introduction

Digital holography has more than 50 years old, although, due to its structural advantages, it is still one of the modern 3D imaging technologies. In recent years, researchers have focused on the practical implementation of this 3D technology [1,2]. Also, with the growth of electronic equipment and computer hardware, it has been possible to implement 3D imaging feasibly.
There are two leading distinct technologies in 3D holographic technology that are important to researchers. One is optimal compression and transfer of 3D images to reduce the data volume, and the other is the computational time and burden in coding and decoding 3D images [3]. With the invention of the laser source in 1960, the practical implementation of holography was made possible. Holography requires a single-frequency, single-phase light source that can easily be provided by laser technology. The laser beam enables to capture depth details of a scene, enabling this information transformation to a suitable medium generating a 3D image [2]. It took almost thirty years after the invention of laser light to produce, process, and record acceptable digital holograms using Spatial light modulators and suitable modern computing hardware resources to become available. With the advent of affordable computing power and large capacity media storage, the variety of hologram applications has expanded into many industries such as the Internet and cyberspace, electron microscopes, interferometry, remote sensing and virtual reality [4]. One of the most critical challenges that holographic images present concerns the high volume of 3D data to be transmitted on limited bandwidth channels and stored in affordable devices. Most 3D image media require online use of holograms, making real time 3D compression algorithms particular interesting in the field of holography. It should be noted that conventional 2D compression methods over 3D images may not perform well, because they have not properly addressed the depth compression problem [5].
There are three different ways to store and display holographic images [6]:

– **Brightness-based:** standard imaging where a holographic image is recorded using 3 phases shifted interferograms, and the recorded hologram is extracted directly from its physical equations. In this standard, three 2D

arrays must be stored for each hologram, creating a high volume of data storage and difficulty in the storage of 3D holographic images.
- **Use a phase shift concept:** In this case, the 3D Object is modelled as a light wave that includes two different signals with different phases. Instead of using three 2D matrices, this format requires two 2D matrices for storage, as different signals are equivalent to reverse phase intermediaries. Although the capacity of this standard is less than Brightness-based standard, it is not commonly used for storing and displaying 3D holograms because of the complexity of required computations.
- **Complex format:** In this case, the three-dimensional hologram is stored as a complex number, using 2D complex matrices that takes up twice as much memory on a computer in comparison to a real matrix. Since the complex number can be stored in either real or imaginary or amplitude and phase, there are two different formats to store the image in this mode.

Based on the above details, maintaining maximum quality and reducing the required capacity and bandwidth for 3D imaging are among the challenges of this technology. The increasing demand for 3D image technologies and bandwidth limitation makes this challenge very important in the near future. In addition, the compression of 3D images and videos can reduce the barriers to holographic technology and expand this technology.
This article is structured as follows: In the next section, an overview of the previous research is presented. The proposed method is discussed in detail in the third section. In the fourth section, the database, simulated results and their analysis are presented, and, finally, the last section outlines the conclusions.

2 Related works

Compression methods for Holographic images are generally divided into four categories. The first group is focused on computer-generated holograms [7]. In this group, since only part of the holographic data is available and the rest is generated by computer simulation, it is possible to achieve a high compression factor because the input information contains less information than total data. The main disadvantage of these methods is their heavy computational burden at the hologram creation step, so they are not practically efficient and are therefore, not recommended for real applications. The second group compresses complex values of the Holo plane [8]. The third group category is focused on the Object plane [9]. These methods mainly use one or two levels of frequency transformations, such as Fourier, and require less data than the Holo plane methods. However, a properly modulation of depth can make these methods weaker than the Holo plane methods for depth compression. The fourth category combines Holo and Object plane to perform compression. In such methods, two approaches can be performed depending on the surface and depth of the Object. If the surface moves to a shallow surface, methods

based on Object plane are used, and if the surface is deep, frequency transforms or similar operators are used in the Holo plane [8].
Due to the different applications in Holo and Object plane, the proposed approach is focused on both planes for compression.
Various studies have only focused on Hologram compression methods, including frequency-time transformations, such as wavelet and Fourier transform, and methods that use hybrid codecs such as HEVC, AV1 and VP9. Hybrid codecs use frequency transforms, time-domain operators and feedback blocks to compress and compensate compression error simultaneously, increasing output performance. The wavelet transform is one of the main operators belonging to the time-frequency transformations and has been used to compress holographic images. Due to wavelet suitability for 2D image compression, this transform was tested on holograms using various conditions in the Holo and Object plane. For example, Ali et al. [10], used a wavelet methodology to compress digital holographic images. This research showed that wavelet transform generally has better compression rate than frequency transformers such as Fourier. In addition, the results showed that Haar wavelet is better than other types of wavelet and can be used as a general and efficient wavelet type for 3D image compression.
Viswanathan et al. [11] studied view-dependent compression in holographic images using Gabor wavelets and Fresnelets and showed that the Gabor wavelet has better time-frequency localization than Fresnelet. Blinder et al. [12] studied the JPEG2000 method as a very efficient 2D method in 3D holographic image compression. The JPEG2000 efficiency has been evaluated in compressing holograms in the field of microscopy. Blinder et al. analyzed the impact of different parameters of the JPEG2000 on the quality and time of the compression on holographic images. Xing et al. [13] proposed an adaptive non separable vector lifting scheme for digital holographic data compression on the Holo plane. It explores different algorithms such as spatial feature extraction, feature vector formation and correlation between these vectors, to perform 3D image compression. The obtained results were not compared to wavelet-based methods, but compression parameters and their effect on the quality and run time of some types of holograms were investigated. Viswanathan et al. [14] dealt with wavelet compression and proposed an adaptive model to improve quality and optimize structure in decoding step. It explores the Morlet wavelet in addition to Gabor wavelet. Blinder et al. [15] suggested a phase compression method that compressed holographic images in the phase domain. By using reversible modulo operators, the number of coefficients that need to be unwrapped is significantly reduced, reducing the computational burden of the system. The authors tried to decrease the computations in the compression step without any loss in output quality.
Blinder described how to present hologram formats on hologram displays and discussed modern hologram compression methods such as wavelet transforms, JPEG2000 and Gabor filter [16]. HEVC and AVC were the main codecs used, and the performance of these two codecs on some hologram images was compared. Birnbaum et al. [17] compressed holographic images using atom-wavelet

transforms on macroscopic holograms. The results showed that atom wavelet transform due to its properties can exhibit good compression performance in macroscopic nearfield holograms when the Fresnel number is correctly calculated. The proposed method works based on the specific phase change of near field macroscopic images and is weak in other hologram types. A comparison of the properties of holograms in the Holo plane and Object plane was done in different domains by Bernardo et al. [9]. Compression methods were compared concerning storage, display system and compression rate. As mentioned, the Object plane can be used in some cases instead of the Holo plane. The advantage of Object plane versus Holo plane concerns its ability to display holograms on conventional 2D displays and use operators for processing 3D images similar to the ones used with conventional 2D images.

Various hologram codecs were compared by Peixeiro et al. [6]. HEVC showed the best results on hologram compression and was selected as the best method. In the meantime, Peixeiro et al. proposed an adaptive conversion-based approach codec that exhibited better quality than conventional HEVC codecs by learning the specific conditions. Particularly, the modified codec showed better compression performance than standard HEVC. Finally, in a review article, Blinder et al. [18], was identified different approaches to holographic coding, recording and display systems.

The authors studied hologram signal processing tasks from different aspects and showed that compression is still a challenging topic and future systems need to perform more compression on holograms based on bandwidth limitations. Bernardo et al. [19] suggested a lossy compression scheme for object plane holograms in the amplitude phase form using HEVC and a preprocessing step to reduce speckle noise of amplitude part of hologram data. Shimobaba et al. [20] used a deep neural network to compress dynamic range in digital holograms. Ko et al. [21] suggested a similar compression scheme to [20] using deep learning, but in Phase-only Holograms. Muhamad et al. [22] addressed some challenges related to holographic coding and standardization. Kim et al. [23] proposed a hybrid zerotree-adaptive discrete wavelet transform for full-complex hologram compression. Hajihashemi et al. [24] combined HEVC, Wavelet, and nearest-neighbour interpolation in a two hierarchical scheme and proposed a new holography image compression method. Their method has been tested on different types of holograms, and its efficiency has been confirmed.

According to those aforementioned, there is a lot of research done on holographic images for compression, but still exist many open challenges in this topic. Content-based compression methods that enhance compression efficiency using content properties are a missing topic in hologram compression. The difference between Holo plane and Object plane, and between real-imaginary and amplitude-phase forms of coded data, cause limited or specific compression schemes that only compressed one type of coded data. The Cartesian storage mode (real and imaginary) has less computational load due to its simplicity, although in some cases, it is weaker in noisy conditions than polar form (amplitude and phase) [25].

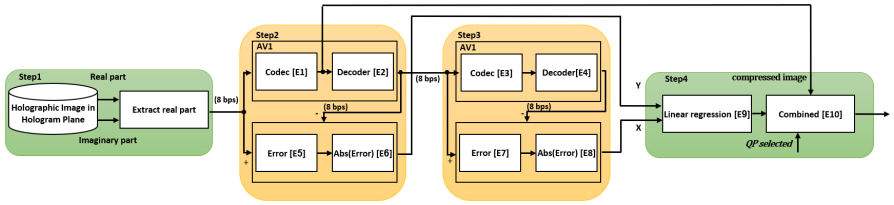

Fig. 1: Encoding steps of the proposed method.

Algorithm 1: Encoding steps

Input: Holography image (Complex Raw data) H_i

Result:

1. Separate real and imaginary parts (R_H and I_H)
2. Apply AV1 codec (with Q_P quantization value) to real and imaginary parts (R_{EH}; I_{EH})
3. Decode outputs (R_{D_EH}; I_{D_EH})
4. Error Calculation between Input data and Decoded Output ($er_{ER} = R_H - R_{D\_EH}$; $er_{EI} = I_H - I_{D\_EH}$)
5. Apply AV1 codec to Decoded outputs (with QPselected quantization value) (R_{ED_EH}; I_{ED_EH})
6. Decode outputs ($R_{D\ ED\_EH}$; $I_{D\ ED\_EH}$)
7. Error Calculation between first and second Decoded outputs ($er_{EER} = R_{D\_EH} - R_{D\_ED\_EH}$; $er_{EEI} = I_{D\_EH} - I_{D\_ED\_EH}$)
8. compute linear relationship between absolute value of er_{EER} and er_{ER} ($|er_{ER}| = m_R \times |er_{EER}| + b_R$)
9. compute linear relationship between absolute value of er_{EEI} and er_{EI} ($|er_{EI}| = m_I \times |er_{EEI}| + b_I$)
10. Send $QP_{selected}$;m_R; b_R;R_{EH};m_I ; b_I ; and I_{EH} to encoding step

---

In most previous researches, such as [18,19,24], it has been shown that HEVC has better performance in comparison with other codecs, and also various researches have been done for optimization of this codec [24]. One of drawbacks of HEVC codec is its being proprietary, which limits its use for commercial purposes. Hence, AV1 codec has been suggested as a free, suitable alternative to this codec. However, its performance is slightly weaker or, in many cases, equal to HEVC; so in this study, the goal was to improve the performance of AV1 codec.

Based on the aforementioned limitations, this article proposes a modified AV1 compression method with the aim of compressing the 3D cartesian form hologram in both Holo and Object planes.
With the same capacity, the proposed method shows higher quality than state-of-the-art 3D image compression codecs. In addition, the proposed method can be used as a general compression method for 2D images.

3 Proposed method

Compression methods are usually divided into compression (encoding) and reading compressed image (decoding) parts. Usually, creating a compressed

file and retrieving it are opposite tasks, but the blocks used on both parts are basically the same, although there are minor differences between them. Details of the proposed compression (encoding) scheme are depicted in (Fig. 1).

3.1 Compression (Encoding step)

After hologram image or video frames enter the system, holograms' real and imaginary parts are separated. The compression block is an AV1 scheme with a selectable quantization coefficient applied to the hologram in E1.
This compressed image is then transferred into two different blocks. The first block decompresses the data using an AV1 decoder in E2, and the second one is directly added to the output file (E10). The output image of E2 is used as input for E5 and E3 blocks. In E5, the decompressed hologram is compared with the original hologram, and the 8-bit error between them is calculated. The absolute value of the output of E5 block is computed in E6. In E3 and E4 blocks, the decoded hologram is compressed and decompressed again using the AV1 method. The Encoder system selects the quantization coefficient of this step.
The output of E4 block is compared with the output image of E2 and the difference between these holograms are extracted as E7 error. The absolute value of E7 is computed as E8. Given the similarity of the standard AV1 method used in E1-E2 and E3-E4 blocks, it is assumed that the error in the first and second encoder-decoder blocks are statistically similar. Based on this assumption, the output of E8 and E6 blocks are used to estimate a linear regression (E9 block) parameter formula. Using the estimated formula in E9, i.e. the image reconstruction step, the proposed method can reproduce absolute of E6 error using E8 and thus, compensate for the error and improve the compression quality. The error sign is assumed to be similar to the two outputs of E5 and E7, so the absolute operator (E6-E8) helps improve the fitting accuracy. The regression coefficients computed at E9, the compressed image at E1 output and the compression coefficient are selected at E3-E4 encoder-decoder and merged into one file in E10. This file is the final output of the proposed compression system. The decompression step first decodes the compressed hologram using the usual AV1 method. The decompressed hologram can be applied to a new AV1 encoder-decoder with selected known quantization coefficient.
Using the obtained value of this step and regression coefficients stored in compressed file, E6 error can be modelled and added to the decompressed hologram to improve the output quality. The regression coefficients and the quantization value, which is used in E3-E4 blocks, are added to the output file. These three values are independent of the size of the holographic image, making the added data to the standard AV1 compressed file negligible. The pseudocode of the compression step (step I) of the proposed method is given in Algorithm 1. Details of the used symbols are given in Table 1.

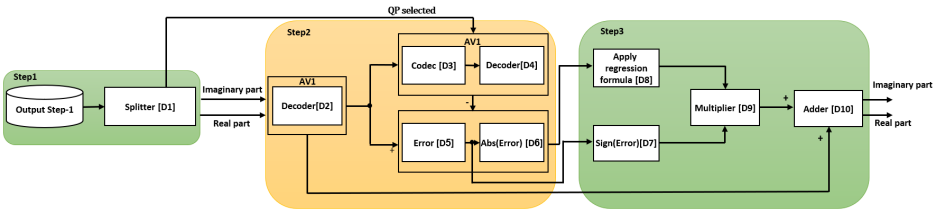

Fig. 2: Decoding step of the proposed method.

Algorithm 2: Decoding steps

Input: Holography image (Complex Raw data) H_i

Result:

1. Separate Compressed real and imaginary parts using AV1 with Q_P (R_{EH}; I_{EH}); $QP_{selected}$ and Two linear relationship formulas (D1)
2. Apply AV1 decoder to R_{EH} and I_{EH} and make R_{D_EH}; I_{D_EH} as Decoded outputs (D2)
3. Apply AV1 codec-decoder to Decoded outputs R_{D_EH}; I_{D_EH} (with $QP_{selected}$ quantization value) and make $R_{D\_ED\_EH}$ and $I_{D\_ED\_EH}$ respectively (D3, D4)
4. Error Calculation between first and second Decoded outputs ($er_{EER} = R_{D\_EH} - R_{D\_ED\_EH}$; $er_{EEI} = I_{D\_EH} - I_{D\_ED\_EH}$)) (D5)
5. Compute absolute value of er_{EER} and er_{EEI} (D6)
6. Compute sign of er_{EER} and er_{EEI} (D7)
7. Apply regression formula (linear relationship) to absolute value of er_{EER} and er_{EEI} and make approximated absolute values of er_{ER} and er_{EI} (D8)
8. Multiply D8 output by the sign of er_{EER} and er_{EEI} to make er_{ER} and er_{EI} to R_{D_EH} (D9)
9. Add er_{ER} and er_{EI} to R_{D_EH}, I_{D_EH} and make compensated output images $\tilde{R}_H$ and $\tilde{I}_H$ (D10)

3.2 Decoding step

In the decoding step, the compressed file is read and then the original file is reconstructed based on it. The decoding steps are exactly the inverse of the compression ones, and the relationships and formulas are usually inverted to reconstruct the original image from the compressed form. In the first block, the compressed file must be split into selected quantization coefficient (QP), linear regression formulas, and compressed real and imaginary parts of hologram. The steps for decoding the real and imaginary parts are similar and acting similarly for the rest. In the second block, the encoded real/imaginary part is decoded, and the standard AV1 image is built as depicted in (Fig. 2).

The decoded part (D2) is applied to an AV1 encoder-encoder block (D3D4) with selected quantization coefficient, and the output image goes to the next step. This D4 output is the same as E4 output of the compression step. The difference between D4 and D2 images is calculated on D5, and then the error sign (D7) and its absolute value (D6) are obtained. D6 output is similar to E7

Table 1: Meanings of the used symbols

Symbols	Meanings
H_i	Input Holography image
R_H	Real part of Input Holography image
I_H	Imaginary part of Input Holography image
QP	Quantization value selected by user
R_EH	Compressed real part using AV1 with QP
$R_{D\_ED\_EH}$	Decompressed Holography real part after main AV1 step
er_ER	Error of main AV1 compression in real part
I_EH	Compressed imaginary part using AV1 with QP
I_{D_EH}	Decompressed Holography imaginary part after main AV1 step
er_EI	Error of main AV1 compression in imaginary part
$QP_selected$	Quantization value of secondary AV1 step
R_{ED_EH}	Compressed real part in secondary step
$R_{D\_ED\_EH}$	Decompressed real part Holo image after secondary step
I_{ED_EH}	Compressed imaginary part in secondary step
$I_{D\_ED\_EH}$	Decompressed imaginary image after secondary step
er_EER	Error of secondary step belong to real part
er_EEI	Error of secondary step belong to imaginary part
M_R	Slope of linear equation between er_{EER} and er_{ER} (see encoding pseudocode)
b_R	$\lvert er_{ER}\rvert$ intercept in linear equation between er_{EER} and er_{ER}
M_I	Slope of linear equation between er_{EEI} and er_{EI} (see encoding pseudocode)
B_I	$\lvert er_{EI}\rvert$ intercept in linear equation between er_{EEI} ander_{EI}
$\widetilde{er}_{ER}$	Approximated value of er_{ER} in decoder block
$\widetilde{er}_{EI}$	Approximated value of er_{EI} in decoder block
$\widetilde{R}_H$	Approximated value of R_H in decoder block
$\widetilde{I}_H$	Approximated value of I_H in decoder block

output of the compression step and is applied as input to the regression formula. The other input of D8 block is linear regression of E9 block (compression step) that split the input file in the first block. D8 block calculates the error between the original image and the decoded hologram using linear relationship and the result is obtained in D6. This block is an error compensation block. If the relationship was perfect when using this compensator, the original image would be ideally restored, but this will not occur due to the special, non-linear nature of the AV1 scheme. The error calculated in D8, which is equivalent to E6 output, is equal to absolute error. This value is multiplied by the error sign (D7) in the multiply block (D9) and forms the final error.

The proposed method assumes that D5 and E5 signs are exactly the same, but this assumption is violated in some cases. In D10 block, the computed final error is added to the output image D2. If D5 and E5 errors are similar and the relationship between the two errors is partially linear, the compensator block will be able to compensate the error in both the real and imaginary parts of the hologram. The above steps for both real and imaginary parts are similar, with two different linear formulas added separately to the output file. Only the selected QP is similar for the real and imaginary parts. However, the use of unequal quantization coefficients can also be considered when it becomes necessary. Using this compensator and without considerable change in the size of the encoded file, the image quality of the proposed method will

Table 2: Hologram Characteristics

	Resolution (pixel)	**Pixel pitch (µm)**	**Reconstruction distance (m)**	**Wavelength (nm)**
3D-Multi	1920×1080	8	0.51, 0.50, 0.49	632.8
2D-Multi	1920×1080	8	0.51, 0.50, 0.49	632.8
3D-Venus	1920×1080	8	0.50	632.8
Car2575	600×600	4.4	0.245	632.8
Cube	972×972	4.4	0.135	632.8
King	972×972	4.4	0.14	632.8
Dice2	2588×2588	2.2	0.1595	632.8
Skull	2588×2588	2.2	0.1690	632.8
Astronaut	2588×2588	2.2	0.1721	632.8

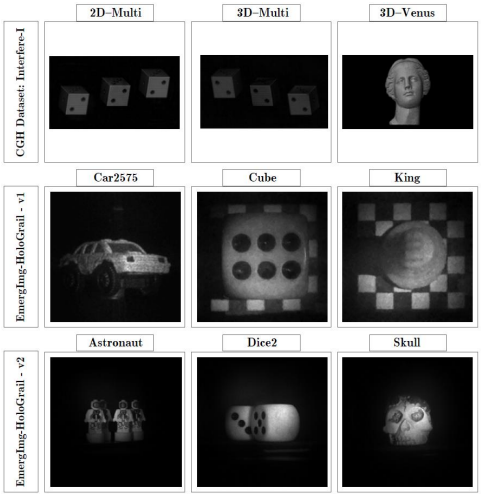

Fig. 3: 2D representation of the selected testing holograms.

be better than the one of the standard AV1. The decoding pseudocode is given by Algorithm 2, where the used symbols have the meanings given in (Table. 1).

4 Experiments

4.1 Database

To confirm the performance of the proposed method, the method was evaluated on two hologram types belong to two different databases.

4.1.1 EmergIMg

The first used database is EmergIMg (EmergImg-HoloGrail - v1 & 2) [26, 27], which contains a total of 10 holographic images that can be divided into two separate groups in terms of dimension. As the included holograms were recorded under real conditions, all of them contain noise and distortion.

4.1.2 Interfere

Interfere-I is the second database that was used in the experiments. This database contains 5 images with different dimensions and was created under the scope of Peter Shelkens's research group [28] using simulation software, so we refer to this dataset as computer-generated holographic database (CGH). The computer-generated holograms are very different from the real ones included in the EmergIMg database. It should be noted that only the real and imaginary parts of the selected holograms were used to evaluate the proposed method. Nine holograms from two used datasets were selected. Fig. 3 shows the 2D shape of the selected holograms, while the specifications of each of them are given in Table 2).

4.2 Standard Coding Solutions

Many compression algorithms have been suggested for 3D image compression. Most of them are a copy of successful 2D versions. The state-of-the-art 3D compression methods that were selected for comparison were JPEG2000, H265, AV1 and VP9, which are introduced in this section.

4.2.1 JPEG 2000

JPEG is one of the most commonly used lossy compression formats for digital images. Users can choose the compression ratio of JPEG as a selectable parameter for obtaining the lowest storage size versus the acceptable image quality. It uses several mechanisms to keep the region of interest better at varying the degrees of granularity. Kakado [29] software was used for the JPEG 2000 implementation.

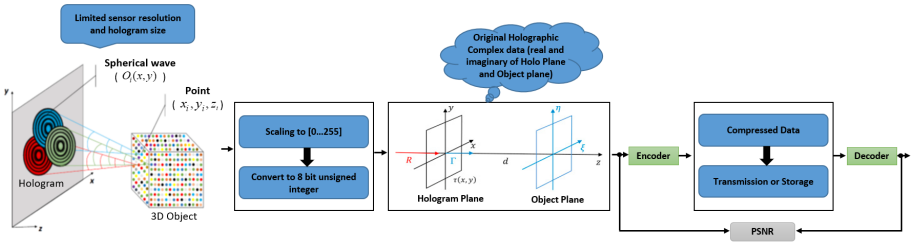

Fig. 4: Block diagram of the used quality assessment scheme.

4.2.2 HEVC Intra

High Efficiency Video Coding (HEVC), also known as H.265, is one of the best current 2D and 3D compression formats. This format uses discrete cosine and sine transforms and enhances 25 to 50% compression efficiency relative to the basic HEVC. In comparison to other compression standards, HEVC improves the video quality at the same bit rate. This research was performed using the standard HEVC codec implemented in [30]. Based on the codec input data requirements, the Main hologram profile was converted to 4:0:0 data from its original (4:2:0).

4.2.3 AOM / AV1

AOMedia Video 1 (AV1) codec was designed as an open, royalty-free compression format, mainly for Internet [31]. The main goal of the AV1 designing was to make it a free commercial use, open source codec for all platforms [32]. According to [33], the main difference between AV1 and VP9 is some in-loop filters that reduce the quality loss and increase the output quality.

4.2.4 VP9

Like AV1, VP9 is a royalty-free block-based compression format created by Google for YouTube platform and is currently supported and enhanced by Google. Many comparisons have been done between VP9 and HEVC [34]. Briefly, VP9 is weaker than HEVC, but the gap between VP9 and HEVC is reduced or even reversed by setting encoding parameters accurately. One of the other advantages of VP9 format compared to HEVC concerns its simple bitstream and fewer blocks than HEVC.

5 Results and Discussion

In this section, simulation results are given according to the selected databases and codecs. All simulations were performed under the same assumptions used

in the similar blocks of different codecs. The results for the real and imaginary parts of the holographic images in the Holo and Object planes are given separately using diagrams and tables to show the efficiency of the proposed method relative to the existing methods under comparison. The block diagram of the comparison scheme is shown in Fig. 4. As can be observed, the real and imaginary parts of the hologram (system input) were assumed in the Cartesian space. The two real and Imaginary parts were separately mapped to a range of 0 to 255, and then converted to 8-bit unsigned integers. In the next step, the converted images were compressed using state-of-the-art codecs and proposed method and the quality achieved by each method was assessed by comparing the original image with the compressed one. The metrics used in the quality assessment were: peak signal-to-noise ratio (PSNR) [6,19], structural similarity index (SSIM) [35,19], Bjøntegaard delta PSNR (BD-PSNR) and BD-Rate [19,24], which were computed separately for all selected images in both real and imaginary parts in order to highlight that the proposed method works well in all types of holograms.

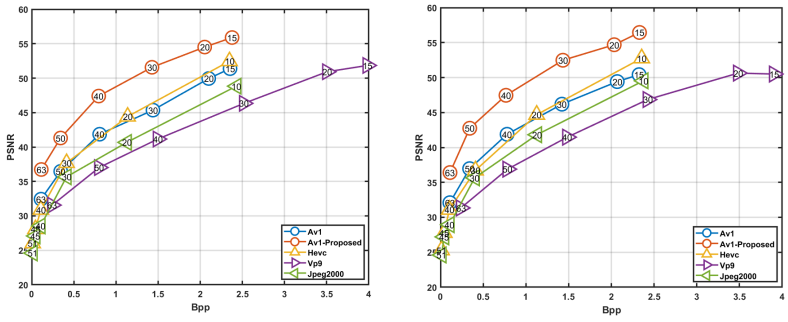

Fig. 5: PSNR vs bits per pixel (bpp) in the real part (left) and imaginary part (right) as to the 3Dmulti hologram (HP) for the different codecs under comparison.

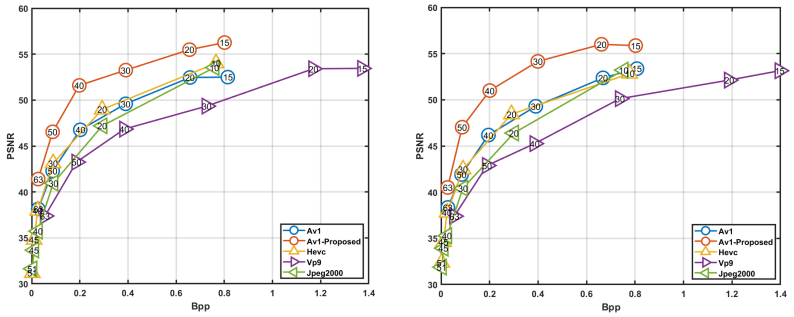

Fig. 6: PSNR vs bpp in the real part (left) and imaginary part (right) as to the 3Dmulti hologram (OP) for the different codecs under comparison.

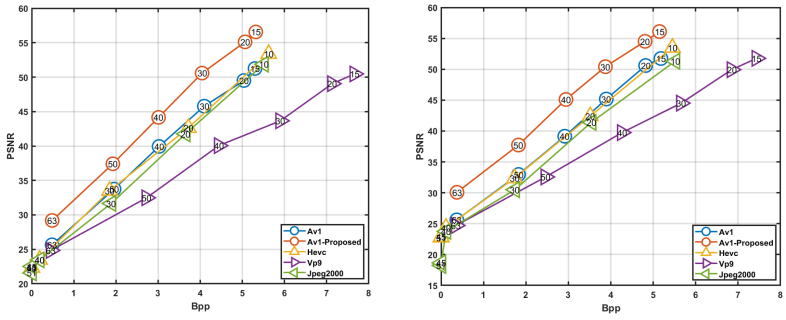

Fig. 7: PSNR vs bpp in the real part (left) and imaginary part (right) as to the Cube hologram (HP) for the different codecs under comparison.

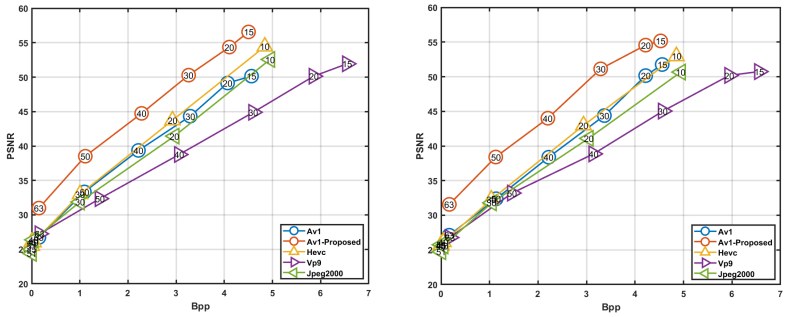

Fig. 8: PSNR vs bpp in the real part (left) and imaginary part (right) in Cube hologram (OP) for different codecs under comparison.

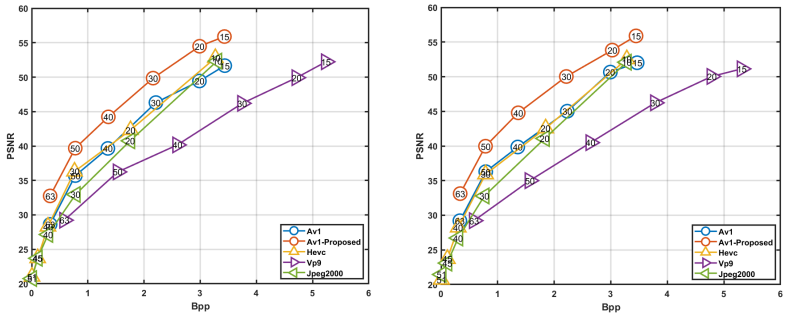

Fig. 9: PSNR vs bpp in the real part (left) and imaginary part (right) as to the Astronaut hologram (HP) for the different codecs under comparison.

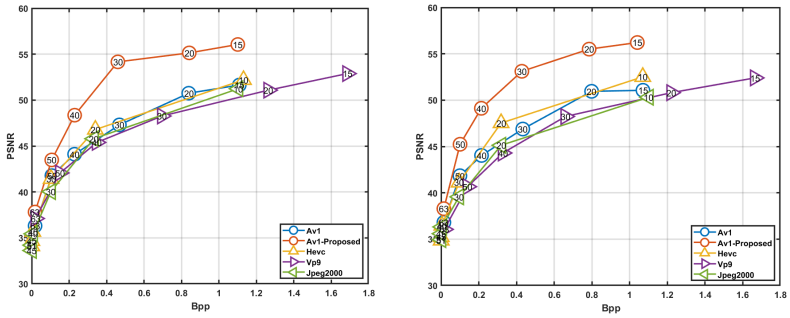

Fig. 10: PSNR vs bpp in the real part (left) and imaginary part (right) as to the Astronaut hologram (OP) for the different codecs under comparison.

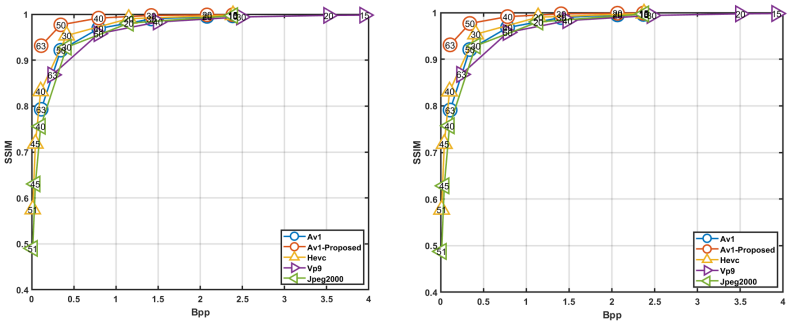

Fig. 11: SSIM vs bpp in the real part (left) and imaginary part (right) as to the 3Dmulti hologram (HP) for the different codecs under comparison.

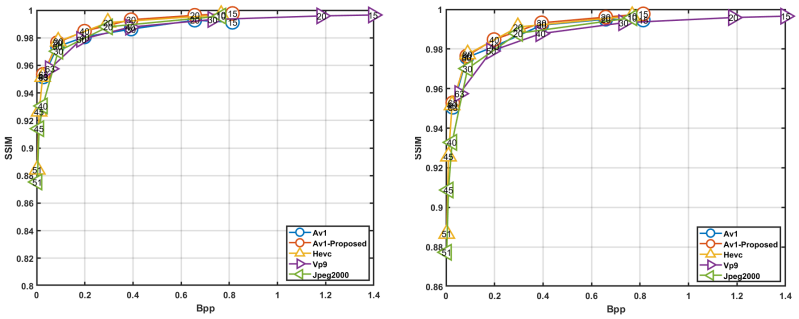

Fig. 12: SSIM vs bpp in the real part (left) and imaginary part (right) as to the 3Dmulti hologram (OP) for the different codecs under comparison.

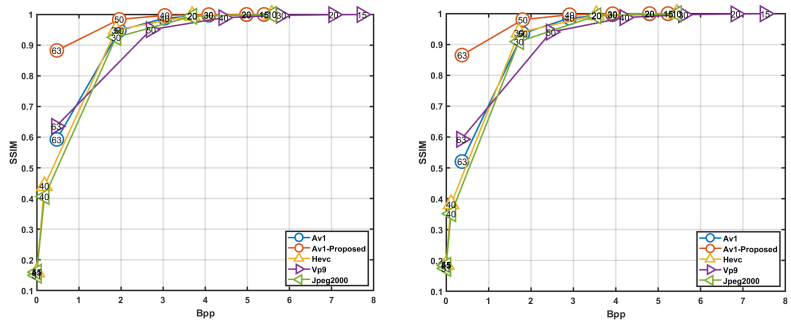

Fig. 13: SSIM vs bpp in the real part (left) and imaginary part (right) as to the Cube hologram (HP) for the different codecs under comparison.

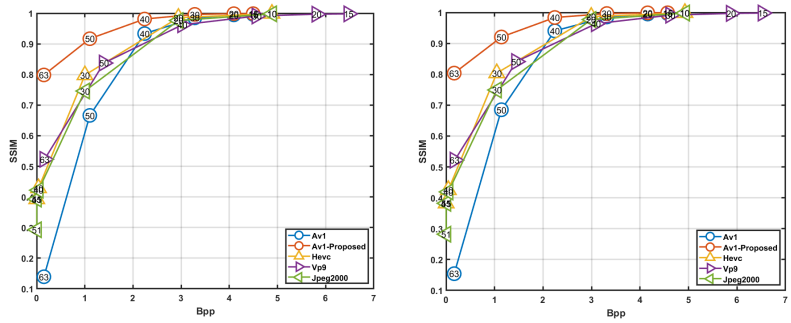

Fig. 14: SSIM vs bpp in the real part (left) and imaginary part (right) as to the Cube hologram (OP) for the different codecs under comparison.

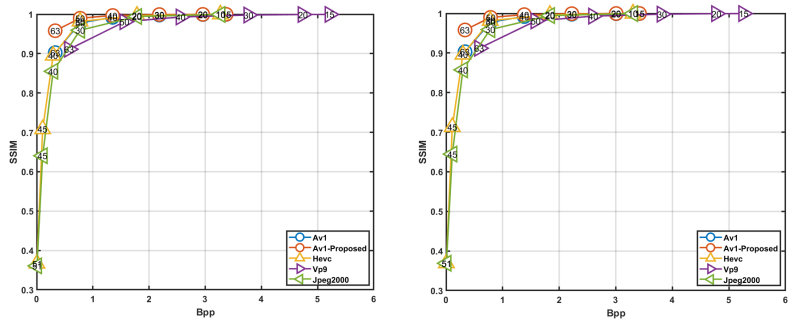

Fig. 15: SSIM vs bpp in the real part (left) and imaginary part (right) as to the Astronaut hologram (HP) for the different codecs under comparisons.

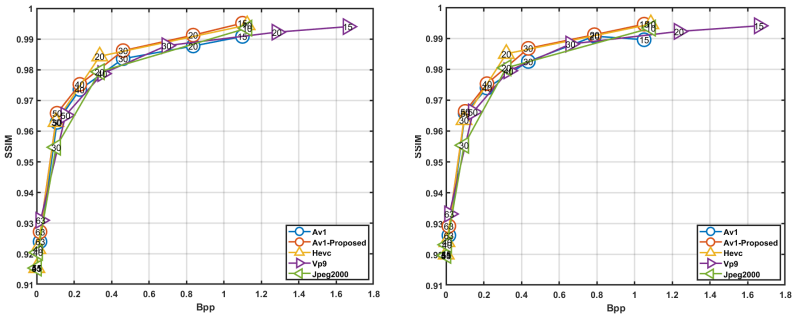

Fig. 16: SSIM vs bpp in the real part (left) and imaginary part (right) as to the Astronaut hologram (OP) for the different codecs under comparison.

Table 3: Relative performance of the proposed method.

	Imaginary (Holo Plane)		**Imaginary (Object Plane)**	
3D-Multi	**BD-PSNR**	**BD-Rate**	**BD-PSNR**	**BD-Rate**
	5.1545	-56.0328	3.5959	-55.8921
	Real (Holo Plane)		**Real (Object Plane)**	
	BD-PSNR	**BD-Rate**	**BD-PSNR**	**BD-Rate**
	5.1528	-55.8297	3.5743	-55.6578
2D-Multi	**Imaginary (Holo Plane)**		**Imaginary (Object Plane)**	
	BD-PSNR	**BD-Rate**	**BD-PSNR**	**BD-Rate**
	5.1888	-64.0886	3.8441	-63.4664
	Real (Holo Plane)		**Real (Object Plane)**	
	BD-PSNR	**BD-Rate**	**BD-PSNR**	**BD-Rate**
	5.1775	-62.5350	3.1518	-47.3675
3D-Venus	**Imaginary (Holo Plane)**		**Imaginary (Object Plane)**	
	BD-PSNR	**BD-Rate**	**BD-PSNR**	**BD-Rate**
	5.1869	-63.4676	3.6201	-52.0219
	Real (Holo Plane)		**Real (Object Plane)**	
	BD-PSNR	**BD-Rate**	**BD-PSNR**	**BD-Rate**
	5.1912	-66.8596	3.6052	-52.5266
Cube	**Imaginary (Holo Plane)**		**Imaginary (Object Plane)**	
	BD-PSNR	**BD-Rate**	**BD-PSNR**	**BD-Rate**
	3.8198	-35.5501	4.1287	-44.2570
	Real (Holo Plane)		**Real (Object Plane)**	
	BD-PSNR	**BD-Rate**	**BD-PSNR**	**BD-Rate**
	3.9674	-33.3561	4.0431	-45.1494
Horse	**Imaginary (Holo Plane)**		**Imaginary (Object Plane)**	
	BD-PSNR	**BD-Rate**	**BD-PSNR**	**BD-Rate**
	4.6003	-25.2420	4.4186	-43.1818
	Real (Holo Plane)		**Real (Object Plane)**	
	BD-PSNR	**BD-Rate**	**BD-PSNR**	**BD-Rate**
	4.5439	-26.2485	4.4061	-40.9431
Car2575	**Imaginary (Holo Plane)**		**Imaginary (Object Plane)**	
	BD-PSNR	**BD-Rate**	**BD-PSNR**	**BD-Rate**
	4.4479	-35.6332	4.2779	-57.9580
	Real (Holo Plane)		**Real (Object Plane)**	
	BD-PSNR	**BD-Rate**	**BD-PSNR**	**BD-Rate**
	4.4165	-34.2359	4.2122	-57.9678
Skull	**Imaginary (Holo Plane)**		**Imaginary (Object Plane)**	
	BD-PSNR	**BD-Rate**	**BD-PSNR**	**BD-Rate**
	3.8798	-31.3506	3.2588	-47.8609
	Real (Holo Plane)		**Real (Object Plane)**	
	BD-PSNR	**BD-Rate**	**BD-PSNR**	**BD-Rate**
	3.8774	-31.5212	3.2684	-48.1116
Astronaut	**Imaginary (Holo Plane)**		**Imaginary (Object Plane)**	
	BD-PSNR	**BD-Rate**	**BD-PSNR**	**BD-Rate**
	3.9621	-32.5947	3.0875	-56.6582
	Real (Holo Plane)		**Real (Object Plane)**	
	BD-PSNR	**BD-Rate**	**BD-PSNR**	**BD-Rate**
	3.9651	-32.8290	3.0383	-54.2671
Dice2	**Imaginary (Holo Plane)**		**Imaginary (Object Plane)**	
	BD-PSNR	**BD-Rate**	**BD-PSNR**	**BD-Rate**
	3.8934	-28.8868	3.3292	-50.5337
	Real (Holo Plane)		**Real (Object Plane)**	
	BD-PSNR	**BD-Rate**	**BD-PSNR**	**BD-Rate**
	3.8992	-29.1711	3.4726	-52.9819

The computational platform used in the experiments was Matlab 2020a. The used values for the quantization coefficient of the standard AV1 were 63, 50, 40, 30, 30, 20 and 15. In VP9, JPEG2000 and HEVC methods, the values of the quantization coefficient were selected according to these values, so the obtained PSNR results versus bpp can be compared against the ones obtained by the proposed method. The PSNR results obtained by each studied method are depicted in Figures 5 to 10. In addition, the proposed method was compared using BD-PSNR and BD-Rate against the basic AV1 method in both real and imaginary parts in all images. The results of this comparison are given in Table 3.

Figures 5 and 6 show the PSNR values as to the real and imaginary parts of the 3DMulti image in the Holo plane and Object plane, respectively. Figures 7 and 8 show the PSNR values as to the real and imaginary parts of the Cube image, and Figures 9 and 10 of the Astronaut image, respectively. As can be observed, the proposed method had a better performance in three different holograms of the used datasets in both Holo and Object planes and in real and imaginary parts compared to the state-of-the-art methods under comparison. By comparing the efficiency of the proposed method against the other methods, the proposed method performed much better in terms of PSNR than HEVC and AV1, which had the best results among the studied related codecs. The difference between PSNR of the proposed method and the other methods in some cases was about 5 dB, which indicates a very good improvement.

In Figures 5 to 10, except the proposed method, the best obtained quality belongs to HEVC and AV1 codecs. Similar results can be observed with slight differences in Cube hologram in Figures 7 and 8 and Astronaut hologram in Figures 9 and 10.

Figures 11 and 12 show the SSIM values as to the real and imaginary parts of the 3Dmulti image in the Holo plane and Object plane, respectively. These figures show that in terms of SSIM, the difference between the proposed method and the other methods under comparison is lower than as to PSNR, but still, the proposed method is better than the other state-of-the-art methods, especially at lower bpp values. For all compression methods, the obtained SSIM values in 3Dmulti (object plane) are approximately similar, so the advantage of the proposed method in Holo plane is more evident. The proposed method shows a significant improvement in Cube image relatively to the other compression methods (Figures 13 and 14), especially for bpp lower than 2. In Astronaut hologram (Figures 15 and 16), the results are similar to those found in 3Dmulti. In terms of SSIM, in all cases, the best compression method after the proposed one was HEVC.

Because point-to-point comparisons in terms of SSIM and PSNR may not show clearly the improvement that can be achieved by the proposed method, the new method and the basic AV1 codec were compared using two relative criteria: BD-PSNR and BD-Rate, so the rate of improvement could be clearly observed. The results of this comparison are reported in Table. 3. From the data in this table, it can be realized that the proposed method has shown considerably better results than the basic method, which indicates once again

its very good performance. The best improvement achieved by the proposed method occurred in terms of BD-PSNR for the 3DMulti imaginary part, which shown an improvement of about 5 dB. The best performance as to BDRate was for the 3DVenus hologram (about 63%). All the findings revealed that the proposed method had better performance than all the compared state-of-the-art methods [4,7,13,19] in the studied holograms.
It should be noted, due to the existence of an extra AV1 codec and decoder in step 3 of encoding and step 2 of the decoding scheme of the proposed method, the speed of encoding and decoding in the proposed method is slower than of the normal AV1 codec.

6 Conclusions

This study proposed a combined method based on two hierarchical AV1 codecs for compression of holographic images. The proposed method is based on the AV1 codec by adding compensatory layers in order to be able to improve its output quality without imposing additional data. In this regard, when compared to the basic AV1 codec, the proposed method significantly improved the quality of the output in the real and imaginary parts of Holo and Object planes. In the meantime, the performance of the proposed method is independent of the type of 3D image generation method (real acquired or computer-generated). Another interesting feature of the proposed method is its stable behavior by increasing the compression rate, which defines a predictable relationship between quality and compression ratio. This relationship in conventional codecs is not predictable in some holograms. The simulation results show that the proposed codec in 3D images at higher compression ratios achieved better quality than the other codecs under comparison. In addition, when compared to the basic AV1 codec, in terms of BDPSNR and BDRate, the proposed codec increased the efficiency up to 63% as to BDRate and 5 dB as to BDPSNR, which indicates the higher suitability of the proposed codec in compressing holograms compae to the AV1 codec. In addition, the proposed method can also be used as a general compression method for 2D images.
Enhancing JPEG2000 codec using the proposed method and using JPEG2000 in the proposed method similar to the work done in [24] with wavelet transform will be considered as future research.

References

1. P. Picart and S. Montresor, "Digital holography," in *Optical Holography*. Elsevier, 2020, pp. 83–120.
2. G. T. Nemetallah, R. Aylo, and L. A. Williams, "Analog and digital holography with matlab." SPIE, 2015.
3. F. Dufaux, Y. Xing, B. Pesquet-Popescu, and P. Schelkens, "Compression of digital holographic data: an overview," in *Applications of Digital Image Processing XXXVIII*, vol. 9599. International Society for Optics and Photonics, 2015, p. 95990I.
4. F. Monroy, *Holography: Different Fields of Application*. BoD–Books on Demand, 2011.

5. T.-C. Poon and J.-P. Liu, *Introduction to modern digital holography: with MATLAB*. Cambridge University Press, 2014.
6. J. P. Peixeiro, C. Brites, J. Ascenso, and F. Pereira, "Holographic data coding: Benchmarking and extending hevc with adapted transforms," *IEEE Transactions on Multimedia*, vol. 20, no. 2, pp. 282–297, 2017.
7. C. Gao, J. Liu, X. Li, G. Xue, J. Jia, and Y. Wang, "Accurate compressed look up table method for cgh in 3d holographic display," *Optics express*, vol. 23, no. 26, pp. 33 194–33 204, 2015.
8. Y. Xing, B. Pesquet-Popescu, and F. Dufaux, "Compression of computer generated hologram based on phase-shifting algorithm," in *European Workshop on Visual Information Processing (EUVIP)*. IEEE, 2013, pp. 172–177.
9. M. V. Bernardo, P. Fernandes, A. Arrifano, M. Antonini, E. Fonseca, P. T. Fiadeiro, A. M. Pinheiro, and M. Pereira, "Holographic representation: Hologram plane vs. object plane," *Signal Processing: Image Communication*, vol. 68, pp. 193–206, 2018.
10. Z. Ali, P. D. Quang, J.-H. Park, N. Kim *et al.*, "Compression of digital hologram for three-dimensional object using wavelet-bandelets transform," *Optics express*, vol. 19, no. 9, pp. 8019–8031, 2011.
11. K. Viswanathan, P. Gioia, and L. Morin, "Wavelet compression of digital holograms: towards a view-dependent framework," in *Applications of Digital Image Processing XXXVI*, vol. 8856. International Society for Optics and Photonics, 2013, p. 88561N.
12. D. Blinder, T. Bruylants, H. Ottevaere, A. Munteanu, and P. Schelkens, "Jpeg 2000-based compression of fringe patterns for digital holographic microscopy," *Optical Engineering*, vol. 53, no. 12, p. 123102, 2014.
13. Y. Xing, M. Kaaniche, B. Pesquet-Popescu, and F. Dufaux, "Adaptive nonseparable vector lifting scheme for digital holographic data compression," *Applied optics*, vol. 54, no. 1, pp. A98–A109, 2015.
14. K. Viswanathan, P. Gioia, and L. Morin, "A framework for view-dependent hologram representation and adaptive reconstruction," in *2015 IEEE International Conference on Image Processing (ICIP)*. IEEE, 2015, pp. 3334–3338.
15. D. Blinder, H. Ottevaere, A. Munteanu, and P. Schelkens, "Efficient multiscale phase unwrapping methodology with modulo wavelet transform," *Optics express*, vol. 24, no. 20, pp. 23 094–23 108, 2016.
16. D. Blinder, "Efficient representation, generation and compression of digital holograms," Ph.D. dissertation, PhD thesis, 2018.
17. T. Birnbaum, D. Blinder, C. Schretter, and P. Schelkens, "Compressing macroscopic near-field digital holograms with wave atoms," in *Digital Holography and Three-Dimensional Imaging*. Optical Society of America, 2018, pp. DW2F–5.
18. D. Blinder, A. Ahar, S. Bettens, T. Birnbaum, A. Symeonidou, H. Ottevaere, C. Schretter, and P. Schelkens, "Signal processing challenges for digital holographic video display systems," *Signal Processing: Image Communication*, vol. 70, pp. 114–130, 2019.
19. M. V. Bernardo, E. Fonseca, A. M. Pinheiro, P. T. Fiadeiro, and M. Pereira, "Efficient coding of experimental holograms using speckle denoising," *Signal Processing: Image Communication*, vol. 96, p. 116306, 2021.
20. T. Shimobaba, D. Blinder, M. Makowski, P. Schelkens, Y. Yamamoto, I. Hoshi, T. Nishitsuji, Y. Endo, T. Kakue, and T. Ito, "Dynamic-range compression scheme for digital hologram using a deep neural network," *Optics letters*, vol. 44, no. 12, pp. 3038–3041, 2019.
21. H. Ko and H. Y. Kim, "Deep learning-based compression for phase-only hologram," *IEEE Access*, 2021.
22. R. K. Muhamad, T. Birnbaum, A. Gilles, S. Mahmoudpour, K.-J. Oh, M. Pereira, C. Perra, A. Pinheiro, and P. Schelkens, "Jpeg pleno holography: scope and technology validation procedures," *Applied Optics*, vol. 60, no. 3, pp. 641–651, 2021.
23. J.-K. Kim, K.-J. Kim, J.-W. Kang, K.-J. Oh, J.-W. Kim, D.-W. Kim, and Y.-H. Seo, "New compression method for full-complex holograms using the modified zerotree algorithm with the adaptive discrete wavelet transform," *Optics Express*, vol. 28, no. 24, pp. 36 327–36 345, 2020.
24. V. Hajihashemi, H. E. Najafabadi, A. A. Gharahbagh, H. Leung, M. Yousefan, and J. M. R. Tavares, "A novel high-efficiency holography image compression method, based

on hevc, wavelet, and nearest-neighbor interpolation," *Multimedia Tools and Applications*, pp. 1–14, 2021.
25. L. Yaroslavsky and J. Astola, "Introduction to digital holography," 2009.
26. D. Blinder, A. Ahar, A. Symeonidou, Y. Xing, T. Bruylants, C. Schretter, B. Pesquet-Popescu, F. Dufaux, A. Munteanu, and P. Schelkens, "Open access database for experimental validations of holographic compression engines," in *2015 Seventh International Workshop on Quality of Multimedia Experience (QoMEX)*. IEEE, 2015, pp. 1–6.
27. E. Fonseca, P. Fiadeiro, V. Hajihashemi, M. Bernardo, A. Pinheiro, and M. Pereira, "Perceptual evaluation of speckle noise reduction techniques for phase shifting holograms," in *2019 Eleventh International Conference on Quality of Multimedia Experience (QoMEX)*. IEEE, 2019, pp. 1–6.
28. P. Schelkens, T. Ebrahimi, A. Gilles, P. Gioia, K.-J. Oh, F. Pereira, C. Perra, and A. M. Pinheiro, "Jpeg pleno: Providing representation interoperability for holographic applications and devices," *ETRI journal*, vol. 41, no. 1, pp. 93–108, 2019.
29. D. S. Taubman and M. W. Marcellin, "Jpeg2000: Standard for interactive imaging," *Proceedings of the IEEE*, vol. 90, no. 8, pp. 1336–1357, 2002.
30. G. J. Sullivan, J.-R. Ohm, W.-J. Han, and T. Wiegand, "Overview of the high efficiency video coding (hevc) standard," *IEEE Transactions on circuits and systems for video technology*, vol. 22, no. 12, pp. 1649–1668, 2012.
31. Y. Chen, D. Murherjee, J. Han, A. Grange, Y. Xu, Z. Liu, S. Parker, C. Chen, H. Su, U. Joshi *et al.*, "An overview of core coding tools in the av1 video codec," in *2018 Picture Coding Symposium (PCS)*. IEEE, 2018, pp. 41–45.
32. D. Grois, T. Nguyen, and D. Marpe, "Coding efficiency comparison of av1/vp9, h. 265/mpeg-hevc, and h. 264/mpeg-avc encoders," in *2016 Picture Coding Symposium (PCS)*. IEEE, 2016, pp. 1–5.
33. J. Valin, "Directional deringing filter," *Internet Draft, Network Working Group, Internet Engineering Task Force*, 2016.
34. D. Mukherjee, J. Bankoski, A. Grange, J. Han, J. Koleszar, P. Wilkins, Y. Xu, and R. Bultje, "The latest open-source video codec vp9-an overview and preliminary results," in *2013 Picture Coding Symposium (PCS)*. IEEE, 2013, pp. 390–393.
35. D. Amirkhani and A. Bastanfard, "An objective method to evaluate exemplar-based inpainted images quality using jaccard index," *Multimedia Tools and Applications*, pp. 1–14, 2021.